



A comparison of electron transfer in ribonucleotide reductase and the bacterial photosynthetic reaction center

Per E.M. Siegbahn^{*}, Margareta R.A. Blomberg, Maria Pavlov

Department of Physics, Stockholm University, Box 6730, S-113 85 Stockholm, Sweden

Received 9 March 1998; in final form 11 June 1998

Abstract

The energy requirements for electron transfer in two different proteins are compared, based on quantum chemical calculations. The methods used are the hybrid density functional B3LYP combined with dielectric cavity models to account for the effects of the polarizable protein. The experimental exothermicities for the electron transfer steps from the chlorophyll special pair both to the pheophytin and to the quinone are well reproduced. For ribonucleotide reductase (RNR), the same methods in contrast predict a large endothermicity for the electron transfer from the cysteine at the substrate site to the tyrosyl radical in the interior of the protein. This indicates that another type of process is active in RNR. Previous work has suggested that this process is hydrogen atom transfer. © 1998 Elsevier Science B.V. All rights reserved.

1. Introduction

Electron transfer (ET) is a common phenomenon in biochemical systems. A good example is the charge separation process in photosynthesis. With the help of a photon, an electron is transferred from chlorophyll, first to a pheophytin and then to a quinone. In the bacterial photosynthetic reaction center, this charge separation process leads to a distance between the charges of 25–30 Å. In another protein, ribonucleotide reductase (RNR), which transforms the ribose residues of the RNA nucleotides to the 2'-deoxyribose residues of the DNA nucleotides, a critical tyrosyl radical is created more than 30 Å away from the substrate active site. The chemical

mode of communication between the tyrosyl radical and the substrate is commonly referred to as electron transfer [1]. In the present Letter these two cases of ET are compared using quantum chemical methods. It is argued, based on thermodynamics, that the processes in the photosynthetic reaction center and RNR are entirely different in nature. This is done by showing that the charge separation in RNR requires too much energy to be a realistic possibility. In other papers an alternative mechanism to ET is described where charge separation is avoided by effectively moving hydrogen atoms, hydrogen atom transfer (HAT) [2,3].

The present knowledge of RNR has been summarized in recent reviews [4,5]. The *Escherichia coli* RNR has been shown to be an $\alpha_2\beta_2$ tetramer that can dissociate into two catalytically inactive homodimers, R1 and R2 [6]. The formation of the tyrosyl radical occurs in R2, while the RNA nucleotide

^{*} Corresponding author.

substrate reactions occur in R1. The X-ray structures of both R1 and R2 have been determined, the one of R2 by Nordlund et al. [7] and the one of R1 by Uhlin and Eklund [8]. Recently, the structure of R1 including a substrate was also determined by Eriksson et al. [9]. These structures indicate that the distance between the active site in R1 and the tyrosyl radical (Tyr¹²²) in R2 is as large as 30–40 Å and that a chain of conserved hydrogen-bonded residues connects these sites [4,5] (see Fig. 1). The active radical at the substrate end of the chain is most likely a cysteine (Cys⁴³⁹). The tyrosyl radical is created by a bis- μ -oxo Fe(IV)–dimer in R2 which abstracts two hydrogen atoms from surrounding residues to become a resting Fe(III)–dimer complex. In this process, two radicals are produced. One of them is destroyed and the other one is the Tyr¹²² radical,

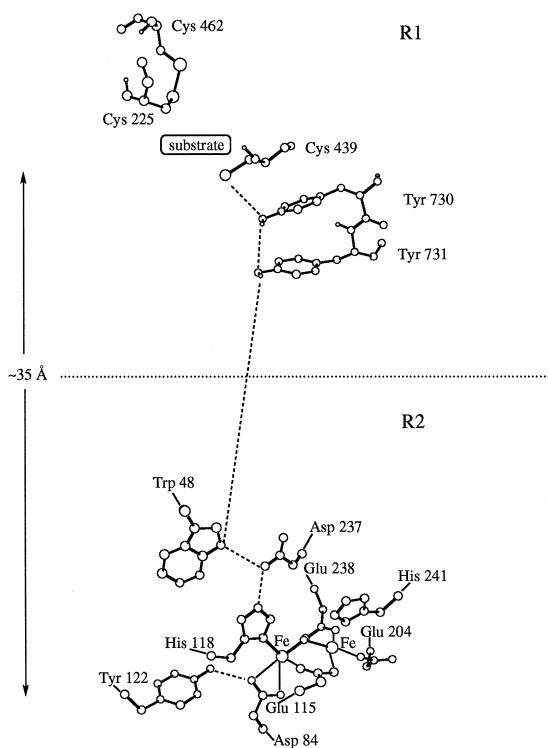


Fig. 1. Conserved residues participating in the proposed hydrogen-bonded long-range transfer chain between the substrate site in protein R1 and the tyrosyl radical in protein R2 of *E. coli* ribonucleotide reductase (RNR). The dashed lines indicate possible hydrogen bonds in the crystal structures of the proteins.

which can be stored for long periods waiting for the substrate to arrive 30 Å away. When, and only when, the substrate arrives will the radical be transferred to the active site Cys⁴³⁹ residue. Site-directed mutagenesis experiments have been interpreted to show that the hydrogen-bonded chain is needed for this radical transfer [10,4].

In the bacterial photosynthetic reaction center, a photon of wavelength 865 nm (*Rhodobacter sphaeroides*) is absorbed by the antenna and the energy is transferred to the chlorophyll special pair leading to the excited state P865*. The energy of this excited state is used to create a charge separation, after 3 ps, where the chlorophyll is ionized to P865⁺, and a nearby pheophytin obtains the electron, forming BPheo_L⁻. The chlorophyll BChl_L, situated in between the special pair and BPheo_L, acts as an intermediate electron carrier. The electron is subsequently, after 200 ps, transferred to the ubiquinone Q_A, forming Q_A⁻. It has been found that the electron always takes this L-branch (to the right in Fig. 2) even though the L-branch is similar. The X-ray structure of the photosynthetic reaction center of *Rhodospseudomonas viridis* (see e.g. Refs. [13–17]).

The hybrid DFT (density functional theory) functional B3LYP is used for the present study [18,19]. Medium-size basis sets are used for the geometry optimizations, while large basis sets are used for the final energies. For benchmark tests comprising 55 common first- and second-row molecules performed using slightly larger basis sets, an average absolute deviation compared to experiments of 2.2 kcal/mol was obtained for the atomization energies, of 0.013 Å for the bond distances and of 0.62° for the bond angles [20]. The present accuracy should be almost as high as in this benchmark test and is enough for the present purposes. For processes like charge separations, it is absolutely necessary to account for long-range polarization effects. This is done here by the dielectric cavity method, both using the SCI-PCM (self-consistent isodensity polarized continuum model) method [21], where the cavity follows the

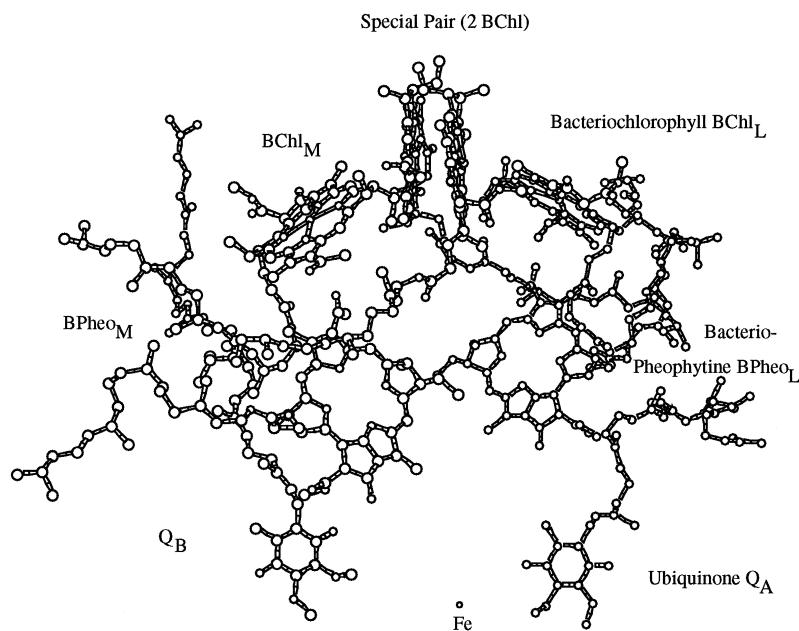


Fig. 2. The photosynthetic reaction center of *Rb. sphaeroides*.

molecular shape and also using a method with an ellipsoidal cavity [22].

2. Computational details

The calculations were performed in three steps. Following an optimization of the geometry, the energy is evaluated using large basis sets, both steps at the B3LYP level. In the third step the effects of the polarized surroundings were evaluated either at the B3LYP or Hartree–Fock level. All calculations were made using the GAUSSIAN94 program [23].

In the B3LYP geometry optimizations a standard double-zeta basis set, the LANL2DZ set of the GAUSSIAN94 program, was used. This rather small basis set can safely be used for the present purposes since it has been clearly shown that the final energy is insensitive to the quality of the geometry optimization [20,24]. The B3LYP energy calculations for the present RNR models were made using the large 6-311 + G(2d,2p) basis sets in the GAUSSIAN94 program. This basis set has two sets of polarization functions on all atoms, and also diffuse functions. For the large chlorophyll models used for the bacte-

rial reaction center, only the LANL2DZ calculation could be afforded. For smaller chlorophyll models it was shown that extensions of the basis sets have only small effects on the relative energies for these systems [12].

The dielectric effects from the surrounding protein were obtained using the self-consistent reaction field (SCRF) method [21,22]. This is one of the simplest models for treating long-range solvent effects and considers the solvent as a macroscopic continuum with a dielectric constant ϵ and the solute as filling a cavity in this continuous medium. In the method of Rivail et al. [22], the charge distribution of the solute is expanded in a series of multipoles, up to sixth-order and the cavity is allowed to be ellipsoidal. An ellipsoidal cavity is still not a good approximation to the shape of many molecules and in some cases even the use of the sixth-order moment is not adequate. In the IPCM (isodensity polarizable continuum) model of Wiberg et al. [21], the cavity is defined in terms of a surface of constant charge density for the solute molecule. The solvent effect is derived from the interactions of the surface potential with the dielectric continuum. This procedure is equivalent to going to infinite-order in the electric

moments. In the present study the self-consistent isodensity polarized continuum model (SCI-PCM) as implemented in the GAUSSIAN94 program has been used. In this method, the solute cavity is determined self-consistently. The default isodensity value of 0.0004 a.u. was used, which has been found to yield volumes close to the observed molar volumes. The dielectric constant of the protein is the main empirical parameter of the model and it was chosen to be equal to 4, in line with previous suggestions for proteins. This value corresponds to $\epsilon \approx 3$ for the protein itself and of $\epsilon = 80$ for the water medium surrounding the protein. It should, in this context, be noted that with such a simple model of the protein surroundings as a dielectric continuum, it is important to include the hydrogen bonding to the solute explicitly in the quantum chemical model. The consequence of this type of modeling can be nicely illustrated by the case of the electron affinity for the quinone in the bacterial reaction center, see further below. Using a quantum chemical model consisting of the quinone and two water molecules embedded in a continuum with $\epsilon = 4$ (see Fig. 3b) an electron affinity of 86.1 kcal/mol is obtained. However, it is generally considered that the region around the quinones in the reaction center is quite polar and therefore has to be described by a high dielectric constant [13]. In fact, using a small quinone model without hydrogen bonding, together with $\epsilon = 80$ gives an electron affinity of 85.0 kcal/mol, close to the value of 86.1 kcal/mol obtained for the model

with hydrogen bonding and $\epsilon = 4$. However, a model treating the most important hydrogen bonding explicitly by quantum chemical methods and assigning a uniform low dielectric constant to the rest of the protein is here considered to be the most appropriate. In the present case, the choice of $\epsilon = 4$ can also be motivated by the fact that this value gives good agreement with experiment for all three charge separation reactions studied in the photosynthetic bacteriosystem [12]. It was also concluded in Ref. [12] that directional effects, which have to be modeled by explicitly charged residues, appear not to be important in this system. RNR is similar to the photosynthetic bacteriosystem in terms of water content and should therefore have a similar dielectric constant. For a discussion of protein modeling see also Ref. [25].

Most of the dielectric calculations were performed at the B3LYP level. However, for the largest chlorophyll models used for the bacterial reaction center (see Fig. 3) this becomes tedious and only the smallest chlorophyll model was used at the B3LYP level. The changes in dielectric effects from extensions of the model from the small to the largest chlorophyll models were obtained at the Hartree–Fock level. It should be noted that the calculated dielectric effect on the absolute ionization potentials and electron affinities are quite similar at the B3LYP and Hartree–Fock level, differing by only 1–2 kcal/mol. Relative effects should be even more similar. When nothing else is said, the dielectric effects included in the values reported below are taken from the SCI-PCM approach. Zero-point vibrational effects were obtained at the B3LYP level and are included in the final values for the RNR systems. Since these effects were found to be small they were not evaluated and assumed to be zero for the bacterial reaction center.

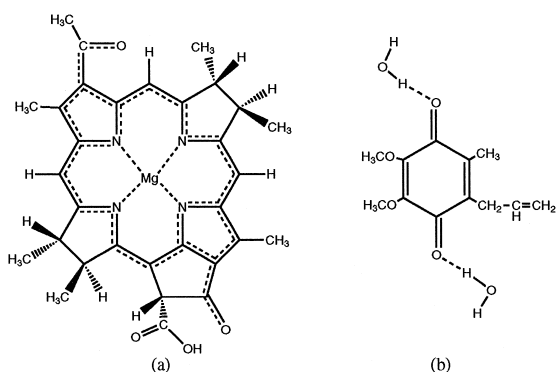


Fig. 3. Models used for BChl (a) and for the ubiquinone (b). The histidine also included in the model, but not shown, is bound to Mg perpendicular to the chlorophyll plane. BPheo is similar to BChl but has two protons instead of Mg^{2+} .

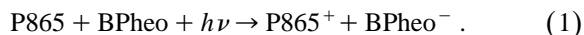
3. Results and discussion

The main purpose of the present study is to investigate whether a charge separation in RNR is energetically feasible. In order to do that the accuracy of the methods used needs to be tested. The biochemical system where the energetics of electron transfer is most accurately known experimentally is

the bacterial photosynthetic reaction center, which was recently studied by the same theoretical methods as used here [12]. Before the RNR results are discussed, the photosynthesis results are therefore briefly repeated.

3.1. Charge separation in the bacterial photosynthetic reaction center

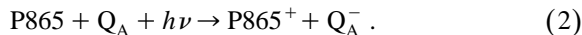
The first step in the charge separation process in the bacterial reaction center is an electron transfer from the special pair to BPheo_L using the energy of a photon of wavelength 865 nm. The process can be written as



Experimentally, this process is found to be exothermic by 5.8 kcal/mol in *Rb. sphaeroides* (see Ref. [15] and references therein). The calculated ionization potential (IP) of the bacteriochlorophyll P865 is 99.5 kcal/mol. To obtain this value the model bacteriochlorophyll shown in Fig. 3a with the peripheral methyl groups and one formyl group replaced by hydrogens was first used. Starting from this smaller model the effects of dimerisation (−5.9 kcal/mol) of peripheral methyl and formyl groups (shown in Fig. 3a; −4.6 kcal/mol) and of the axial histidine ligand (−3.6 kcal/mol) were then calculated and added on to give the final value. Dielectric effects from the surrounding protein of −24.8 kcal/mol obtained using the SCI-PCM method have also been included in the final ionization potential of 99.5 kcal/mol. The corresponding procedure for the electron affinity of BPheo leads to a value of 69.2 kcal/mol, where the peripheral methyl and acetyl effects are −2.9, hydrogen bonding from a glutamic acid +4.3 and the dielectric effects +17.0 kcal/mol. To obtain the final driving force for the electron transfer from the special pair to BPheo, the screened Coulomb attraction ($\epsilon = 4$) has to be added. With a distance between the centers of these groups of about 17 Å this leads to an attraction of 4.9 kcal/mol. Using the photon energy of 33.0 kcal/mol, these results give an exothermicity for the electron transfer of $33.0 - 99.5 + 69.2 + 4.9 = 7.5$ kcal/mol, which agrees well with the experimental value of 5.8 kcal/mol.

In order to obtain the driving force for the elec-

tron transfer from the special pair to the ubiquinone Q_A, the electron affinity of Q_A has to be obtained. The process can be written as



The experimental value for this process is 21.7 kcal/mol for *Rb. sphaeroides* (see Ref. [12] and references therein). The model used for Q_A is shown in Fig. 3b, where two water molecules were used to describe the hydrogen bonding to the surrounding protein suggested by the X-ray structure. The calculated electron affinity is 86.1 kcal/mol, where the dielectric effects of +20.9 kcal/mol and the hydrogen-bonding effects of +10.3 kcal/mol are included. (See also the discussion in Section 2.) In this case the screened Coulomb attraction is only 2.8 kcal/mol. Together with the photon energy of 33.0 kcal/mol, the driving force becomes $33.0 - 99.5 + 86.1 + 2.8 = 22.4$ kcal/mol, in fortuitously good agreement with the experimental value of 21.7 kcal/mol. In the gas phase, the charge separation process would instead be endothermic by 14.9 kcal/mol (including the unscreened Coulomb attraction). The calculated dielectric effects from the surrounding protein on this process are thus as large as 37.3 kcal/mol.

In summary for the photosynthetic charge separation, the calculated values are in good agreement with experiments. The calculated driving force for the electron transfer from the special pair to Q_A is 22.4 kcal/mol compared to 21.7 and for the electron transfer from the special pair to BPheo it is 7.5 compared to 5.8 kcal/mol. To some extent this agreement must be considered fortuitous. For the present purpose of comparison to RNR a reasonable accuracy with errors up to 5 kcal/mol is sufficient.

3.2. Charge separation in RNR

The models used to describe a possible charge separation in RNR (shown in Fig. 4), are considerably simpler than those needed for the photosynthetic reaction center. As described in Section 1, the initial step in DNA precursor synthesis by RNR is the creation of a tyrosyl radical at Tyr¹²². This radical is shown by EPR to be neutral and with only weak hydrogen bonding [26,27]. Soon after the RNA nucleotide substrate arrives more than 30 Å away, a

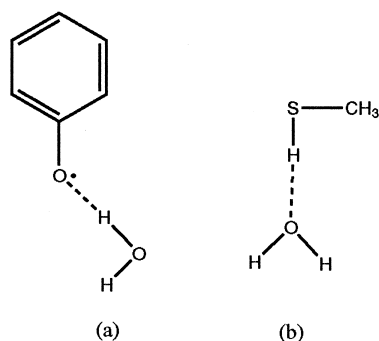
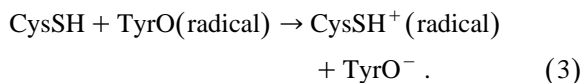


Fig. 4. Models used for the hydrogen-bonded tyrosine Tyr¹²² (a) and for the hydrogen-bonded cysteine Cys⁴³⁹ (b).

hydrogen atom is abstracted probably by a neutral Cys⁴³⁹ radical from the C3' position of the ribose ring [4,9,28,29]. The transfer of radical character from Tyr¹²² to Cys⁴³⁹ could theoretically be by means of electron transfer followed by a local proton transfer to create a neutral cysteinyl radical. This possibility is tested in this study.

The process of electron transfer from Cys⁴³⁹ to Tyr¹²² can be written as



The models used for cysteine and tyrosine are shown in Fig. 4. The gas-phase ionization energy of the isolated cysteine was calculated first. The adiabatic value, obtained as the energy difference between the geometry optimized neutral and ionized states, is 215.7 kcal/mol. This can be compared to the gas-phase value for P865 discussed above, which is 124.3 kcal/mol. It can thus be noted already that the ionization of an amino acid is much harder than the ionization of the special pair–metal complex that is specifically positioned in the photosynthetic reaction center for this purpose. Dielectric effects are as usual important and lower the cysteine ionization potential by 49.4 to 166.3 kcal/mol. The next step, following the procedure described above for the photosynthetic reaction center, is to add possible hydrogen-bonding effects. As indicated in Fig. 1, Cys⁴³⁹ is positioned close to the surface of the protein and has in the 3D structure a hydrogen bond to a tyrosine, Tyr⁷³⁰ [8]. At other stages in the RNR reaction sequence, the

hydrogen bonding could be formed to the OH-bonds of the RNA nucleotide substrate or to water molecules. All these situations should be reasonably well described by using a water molecule as a model. The effect of hydrogen bonding on the adiabatic ionization potential after dielectric effects are added, is a lowering of 7.1 down to 159.2 kcal/mol. This final value can be compared to the much lower value for P865 of 99.5 kcal/mol.

The calculated gas-phase electron affinity of the isolated tyrosyl radical is 51.5 kcal/mol. This value can be compared to the corresponding value for Q_A of 49.8 kcal/mol, showing that on the electron acceptor side the difference is much smaller than for the electron donating side between RNR and the photosynthetic reaction center. Dielectric effects increase the electron affinity of tyrosine by 34.0 to 85.5 kcal/mol. The next step is to add hydrogen-bonding effects. For the case of Tyr¹²², EPR studies indicate that the hydrogen bonding, if any, is weak. Again a water molecule is used to model these effects (see Fig. 4a). The effect of water is 6.1 kcal/mol after dielectric effects are added, leading to a final value for the electron affinity of the tyrosyl radical–water pair of 91.6 kcal/mol to be compared to the corresponding ubiquinone value of 86.1 kcal/mol and the pheophytin value of 69.2 for the photosynthetic reaction center.

Given the above values, the driving force for the electron transfer in RNR can be estimated to be 91.6 – 159.2 = –67.6 kcal/mol, i.e. the process is endothermic. Since this is such a high value, other processes might take place, not taken into account here, such as large motions involving the peptide backbone, which would reduce the value somewhat. If the present models are assumed to be essentially correct, it must be concluded that the same type of radical transfer as in the bacterial photosynthetic system can not occur for RNR. It is perhaps too early to entirely rule out the possibility that the chemical model is not entirely adequate, even though there is nothing at the present stage that points in this direction. To reverse the present conclusions, the model must be totally wrong for RNR and almost perfectly right for the bacterial photosynthetic system, which appears highly unlikely.

The above value calculated for the electron transfer in RNR is based on a simple, but still a reason-

ably realistic, model in line with experimental information of the structure. It is interesting in this context to investigate how different modifications of the immediate environment of Cys⁴³⁹ and Tyr¹²² could have simplified electron transfer. In order to increase the electron affinity of Tyr¹²², a strongly hydrogen-bonding acid should be added. In the experimental structure Asp⁸⁴ is reasonably close (see Fig. 1) but all experimental indications are that it is at most weakly hydrogen bonding to Tyr¹²². Nevertheless, if a formic acid model of Asp⁸⁴ is added instead of the water model used above, the electron affinity of the tyrosyl radical is increased by 13.5 to 73.8 kcal/mol in the gas phase and by 8.7 to 100.3 kcal/mol after dielectric effects are added. This is a substantial effect and has a simple origin. When the electron is added to the tyrosyl radical, the proton affinity clearly increases significantly and a proton is therefore abstracted from the formic acid, leading to a neutral tyrosine. This effect is therefore to a large extent an adiabatic effect due to the change in geometry. However, electron transfer will normally require an almost vertical process in order to avoid high barriers (see below).

In order to simplify electron transfer in RNR further, the environment around Cys⁴³⁹ could also be modified (in theory). The largest effect is reached if a strongly hydrogen-bonding base replaces the water molecule used in the model above. The strongest amino acid base is arginine. The ionization potential of a cysteine–arginine pair is 121.6 kcal/mol including dielectric effects, which is 37.6 kcal/mol smaller than that obtained for the cysteine–water model. If this value is combined with the above result for the phenol–formic acid model, electron transfer now only becomes endothermic by 21.3 compared to 67.6 kcal/mol for the models in Fig. 4. The value of 21.3 must be considered as a hypothetical limit for a cysteine to tyrosyl radical electron transfer in a protein with $\epsilon = 4$.

The above model calculations indicate that an isolated electron transfer in RNR should not occur since the charge separation is too costly. A more accurate description of the protein environment might change the calculated values for the energetics of charge separation somewhat, but the qualitative picture would likely not change. In order to avoid a charge separation between Tyr¹²² and Cys⁴³⁹, a pro-

ton must effectively be moved between the same positions. This argument can be taken even further to conclude that the motion of the electron and the proton must be strongly coupled all the way between the starting point and the end point. In practice this means that instead of an electron transfer there must be a hydrogen atom transfer (HAT) between Tyr¹²² and Cys⁴³⁹. It should be added that this is the only way the charge separation between the two points can be avoided. It can not be avoided by local charge rearrangements at the starting point or at the end point. Different models for HAT have been discussed elsewhere and a typical situation can be sketched as in Fig. 5 with the motion of a hydrogen atom between Tyr⁷³⁰ and Tyr⁷³¹ (see also Fig. 1). The barriers for these hydrogen transfers are less than 10 kcal/mol, for example between two tyrosines and between a tyrosine and a cysteine, corresponding to rates of microseconds and faster.

Since ionization potentials and electron affinities are sensitive to the polarization of the surrounding medium, it is of interest to investigate the dependence of the driving force for electron transfer on the dielectric constant. As a simple estimate of this dependence, the Onsager model [30] can be used. For this model the leading charge term depends on the dielectric constant as $(\epsilon - 1)/2\epsilon$ and contributions from higher moments have a similar dependence. Since the total dielectric effect for process (3) in RNR using the models in Fig. 4 and $\epsilon = 4$ is found to be 76.4 kcal/mol, the effect of going to $\epsilon = 80$ should be an additional 24.2 kcal/mol. When the SCI–PCM model is used to calculate this difference a somewhat larger value of 25.8 kcal/mol is

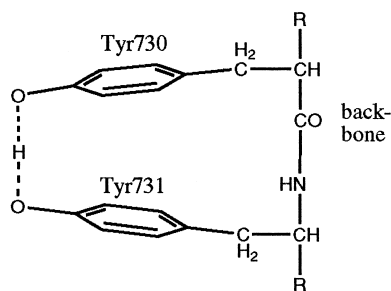
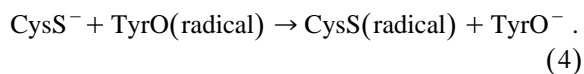


Fig. 5. A sketch of hydrogen atom transfer (HAT) between Tyr⁷³⁰ and Tyr⁷³¹.

found. With the more accurate SCI-PCM value the endothermicity for process (3) for $\epsilon = 80$ becomes 41.8 kcal/mol. This value is substantially smaller than the value calculated for $\epsilon = 4$ of 67.6 kcal/mol, but it is still clear that a straightforward electron transfer between the Cys439 and the Tyr122 residues would not be energetically feasible even in a high dielectric medium.

It should be added that the extrapolation from $\epsilon = 4$ to $\epsilon = 80$, leading to a change of the endothermicity of process (3) from 67.7 kcal/mol to 41.8 kcal/mol, only considers dielectric effects outside of a model that already includes the direct hydrogen-bonding quantum chemically. From the quinone example in Section 2, it is clear that important hydrogen bonding has to be included quantum chemically when a simple dielectric model is used for the protein. Otherwise, if direct hydrogen bonding is not included, it should be obvious from the above examples that a protein can stabilize charges more than water (more than in $\epsilon = 80$). An indication of this is that if an arginine is placed close to the cysteine and a formic acid close to the phenol, process (3) with $\epsilon = 4$ is only endothermic by 21.3 kcal/mol as discussed above, while if no hydrogen bonding is included (a quantum chemical model as in Fig. 4 without the water molecules) and $\epsilon = 80$ is used for the environment, process (3) is much more endothermic with a value of 52.8 kcal/mol for the endothermicity.

As another hypothetical model, the phenol-formic acid pair and the cysteine-arginine pair can be placed in a high dielectric medium with $\epsilon = 80$. For $\epsilon = 4$ this model is endothermic by 21.3 but it actually becomes exothermic with 3.7 kcal/mol for $\epsilon = 80$. As an even more hypothetical model, the cysteine can be regarded as a free anion without any positive counterion in the neighbourhood. If this is the case the electron transfer can be written as



It is obvious already from the onset that this transfer should be much easier than the one described by Eq. (3). The problem is, of course, that in a protein a rather large amount of energy is needed to reach the

starting point for process (4), where the cysteine should be a free anion. This does not mean that cysteine anions do not exist, but they are high in energy, just like hydroxyl anions exist in water even though they cost about 24 kcal/mol to create. For $\epsilon = 4$, process (4) is calculated to be endothermic by 6.8 kcal/mol and for $\epsilon = 80$ it is endothermic by 5.2. To these values the promotion energy to get to the starting point should be added.

Some idea of the sensitivity of the results can be obtained by comparing the dielectric effects obtained using the SCI-PCM method (those given above) to the ones obtained using an ellipsoidal cavity. The dielectric effect on the ionization energy of the cysteine-water pair in Fig. 4b, is -45.1 kcal/mol using the SCI-PCM method. With an ellipsoidal cavity the effect becomes somewhat smaller with a value of -38.1 kcal/mol. For the electron affinity of the tyrosine-water model in Fig. 4a, the dielectric effect is $+31.3$ kcal/mol using the SCI-PCM method and somewhat larger with $+38.3$ using an ellipsoidal cavity. Taken together, these effects lead to a decrease of the endothermicity of reaction (3) by 76.4 kcal/mol using the SCI-PCM method and by exactly the same amount using an ellipsoidal cavity. The conclusion is that for the reaction of interest, reaction (3), the result is practically independent of method used to calculate the dielectric effects of the protein while there is some difference for the absolute values of the ionization potentials and electron affinities. The SCI-PCM values should be regarded as more accurate since the contour of the cavity is allowed to follow the molecular shape better than an ellipsoid one can do. Our experience is that these findings are quite general for these types of processes.

In the initial phase of the present project, an even simpler model of tyrosine was used with a vinyl alcohol molecule rather than a phenol group. These results are reported here to show the low sensitivity of the results to the models used. The calculated gas-phase electron affinity of the vinyl alcohol-water system is 55.0 kcal/mol compared to 60.3 for the phenol system in Fig. 4a. These values become even more similar after dielectric effects are added yielding 89.6 and 91.6 kcal/mol, respectively.

The values discussed above are all adiabatic values, where the geometries have been optimized for

the initial and final states. In order for an electron transfer to be efficient, the molecular rearrangement should be kept as small as possible. The vertical values, without molecular rearrangement, are therefore also of some interest. The vertical electron affinity of the phenol–water system is 88.9 kcal/mol compared to the adiabatic value of 91.6. The difference for the ionization energy of the cysteine–water complex is smaller with a vertical value of 160.8 and an adiabatic value of 159.2 kcal/mol. Taken together, this leads to an endothermicity of process (3) for a vertical process of 71.9 kcal/mol, compared to the adiabatic value of 67.6 kcal/mol.

4. Conclusions

The energy requirement for electron transfer in RNR between the active site cysteine and the tyrosyl radical site in the interior of the protein has been studied by quantum chemical methods. Using a phenol model of tyrosine and an HSCH₃ model of the cysteine, and accounting for hydrogen bonding and dielectric effects, a large endothermicity for ET is predicted. The calculated value is 67.6 kcal/mol. In contrast, for the bacterial photosynthetic reaction center two different ET steps are calculated to be exothermic, in agreement with experiment. In order to achieve an exothermic ET, the photosynthetic reaction center uses the energy of a photon of 33.0 kcal/mol and is also set up to make ET as favourable as possible. As electron donor an easily ionizable chlorophyll molecule is used and as electron acceptor a quinone with a high electron affinity is used. In RNR the tyrosyl radical is a reasonable electron acceptor but the cysteine is quite hard to ionize. In fact, it is much easier to ionize the neighbouring tyrosine residue. Furthermore, if the ionization of the cysteine was the desired process, the protein would at least be set up with a strong base, like an arginine or histidine, close to it. For RNR, electron transfer is furthermore made difficult by the presence of essentially only one path for the transfer. This single hydrogen-bonded pathway is, on the other hand, ideally suited for transferring hydrogen atoms. By keeping the protons and electrons strongly coupled along the transfer, the costly charge separation is avoided in RNR.

Acknowledgements

We are very grateful to Britt-Marie Sjöberg for valuable comments on the manuscript and to Jean-Louis Rivail and Daniel Rinaldi for providing us with their dielectric cavity program.

References

- [1] D. Voet, J.G. Voet, *Biochemistry* (J. Wiley, New York, 1995).
- [2] P.E.M. Siegbahn, M.R.A. Blomberg, R.H. Crabtree, *Theor. Chem. Acc.* 97 (1997) 289.
- [3] P.E.M. Siegbahn, L.A. Eriksson, F. Himo, M. Pavlov, to be published.
- [4] B.-M. Sjöberg, *Struct. Bond.* 88 (1997) 139.
- [5] A. Gräslund, M. Sahlin, *Annu. Rev. Biophys. Biomol. Struct.* 25 (1996) 259.
- [6] P. Reichard, *Science* 260 (1993) 1773.
- [7] P. Nordlund, B.-M. Sjöberg, H. Eklund, *Nature* 345 (1990) 593.
- [8] U. Uhlin, H. Eklund, *Nature* 370 (1994) 533.
- [9] M. Eriksson, U. Uhlin, S. Ramaswamy, M. Ekberg, K. Regnström, B.-M. Sjöberg, H. Eklund, *Structure* 5 (1997) 1077.
- [10] M. Ekberg, M. Sahlin, M. Eriksson, B.M. Sjöberg, *J. Biol. Chem.* 271 (1996) 20655.
- [11] U. Ermler, G. Fritzsche, S.K. Buchanan, H. Michel, *Structure* 2 (1994) 925.
- [12] M.R.A. Blomberg, P.E.M. Siegbahn, G.T. Babcock, *J. Am. Chem. Soc.* in press.
- [13] A. Warsel, Z.T. Chu, W.W. Parson, *Science* 246 (1989) 112.
- [14] R.G. Alden, W.W. Parson, Z.T. Chu, A. Warshel, *J. Am. Chem. Soc.* 117 (1995) 12284.
- [15] M.R. Gunner, A. Nicholls, B. Honig, *J. Phys. Chem.* 100 (1996) 4277.
- [16] M. Marchi, M.E. Gehlen, D. Chandler, M.J. Newton, *J. Am. Chem. Soc.* 115 (1993) 4178.
- [17] M.A. Thompson, M. Zerner, *J. Am. Chem. Soc.* 113 (1991) 8210.
- [18] A.D. Becke, *J. Chem. Phys.* 98 (1993) 5648.
- [19] P.J. Stevens, F.J. Devlin, C.F. Chabrowski, M.J. Frisch, *J. Phys. Chem.* 98 (1994) 11623.
- [20] C.W. Bauschlicher Jr., A. Ricca, H. Partridge, S.R. Langhoff, in: D.P. Chong (Ed.), *Recent Advances in Density Functional Methods, Part II* (World Scientific Publ., Singapore, 1997) p. 165.
- [21] K.B. Wiberg, T.A. Keith, M.J. Frisch, M. Murcko, *J. Phys. Chem.* 99 (1995) 9072.
- [22] V. Dillet, D. Rinaldi, J.-L. Rivail, *J. Phys. Chem.* 98 (1994) 5034.
- [23] M.J. Frisch, G.W. Trucks, H.B. Schlegel, P.M.W. Gill, B.G. Johnson, M.A. Robb, J.R. Cheeseman, T. Keith, G.A. Peters-

- son, J.A. Montgomery, K. Raghavachari, M.A. Al-Laham, V.G. Zakrzewski, J.V. Ortiz, J.B. Foresman, J. Cioslowski, B.B. Stefanov, A. Nanayakkara, M. Challacombe, C.Y. Peng, P.Y. Ayala, W. Chen, M.W. Wong, J.L. Andres, E.S. Replogle, R. Gomperts, R.L. Martin, D.J. Fox, J.S. Binkley, D.J. DeFrees, J. Baker, J.P. Stewart, M. Head-Gordon, C. Gonzalez, J.A. Pople, GAUSSIAN94 Revision B.2, Gaussian, Pittsburgh, PA, 1995.
- [24] P.E.M. Siegbahn, *Adv. Chem. Phys.* 93 (1996) 333.
- [25] A. Warsel, J. Åqvist, *Annu. Rev. Biophys. Chem.* 20 (1991) 267.
- [26] C.W. Hoganson, M. Sahlin, B.-M. Sjöberg, G.T. Babcock, *J. Am. Chem. Soc.* 118 (1996) 4672.
- [27] P.P. Schmidt, K.K. Andersson, A.-L. Barra, L. Thelander, A. Gräslund, *J. Biol. Chem.* 271 (1996) 23615.
- [28] J.A. Stubbe, *Biol. Chem.* 265 (1990) 5330.
- [29] P.E.M. Siegbahn, *J. Am. Chem. Soc.* 120 (1998) in press.
- [30] L. Onsager, *J. Am. Chem. Soc.* 58 (1936) 1486.